Quantum Electronics **48** (9) 813–817 (2018)

https://doi.org/10.1070/QEL16719

Subpicosecond pulse generation above 2 μm in longitudinally inhomogeneous single-mode fibres

I.O. Zolotovskii, D.A. Korobko, V. Rastogi, D.A. Stoliarov, A.A. Sysolyatin

Abstract. **We consider the evolution of the spectrum of a medium-power input telecom laser pulse during propagation in a longitudinally inhomogeneous flattened dispersion silica fibre. Using modelling results, we find an optimal longitudinal fibre diameter profile ensuring transfer of more than 60% of the input pulse energy to a subpicosecond pulse in the range 2.2–2.3 μm.**

Keywords: *light generation in the 2 μm range, longitudinally inhomogeneous optical fibre, supercontinuum generation.*

1. Introduction

The development of laser sources of an optical supercontinuum is one of the major challenges in nonlinear fibre optics [1–3]. It is worth noting that most effort in this area of research has been concentrated on broadband lasing in the visible and near-IR spectral regions. At the same time, applications in tomography, spectroscopy and atmosphere analysis require broadband light at wavelengths above 2 μm [4, 5]. Direct pulse generation in this range is possible with mode-locked holmium [6] or thulium [7] fibre lasers. In the latter case, to reach a wavelength above 2 μm the generated femtosecond pulses should be Raman-shifted by 100 nm or more in the output amplifier. Practical application of such configurations is limited by the fact that specialised fibre-optic components (isolators, lenses, multiplexers, SESAM semiconductor mirrors and others) operating in the range 1.9–2.3 μm are less available and more expensive than standard components of the same quality for the telecom range.

Configurations based on subpicosecond erbium fibre lasers and amplifiers operating in the range 1550–1580 nm are free from these drawbacks. Output pulses of such sources are launched into optical fibre where SRS increases their wavelength to give a broadband supercontinuum. As a rule, specialised fibres are used for supercontinuum generation in the spectral region of interest, e.g. microstructured fibre based on multicomponent oxide glass [5] or ZBLAN fibre [8]. One drawback to this approach is poor compatibility of the specialised fibres with light sources based on standard telecom fibre.

Kamynin et al. [4] and Kurkov et al. [9] investigated supercontinuum generation in the 2 μm range in standard telecom silica fibres and optimised the fibre length. An interesting approach was demonstrated by Anashkina et al. [10]: femtosecond pulses from an erbium fibre source were launched into GeO_2-doped silica fibre to form Raman-shifted fundamental solitons. A distinctive feature of their work was the use of an additional, output fibre with a higher GeO_2 concentration and a lower anomalous dispersion in the fundamental soliton propagation spectrum. The change in dispersion allowed them to use soliton compression and demonstrate broadband supercontinuum generation in the range 1.6–2.5 μm.

Another fibre-optic 'tool', not yet studied in full detail for resolving the problem in question, is longitudinally inhomogeneous fibre with a diameter varying along its length. Investigation of supercontinuum generation in longitudinally inhomogeneous fibre was begun as early as the 1990s [11] and was long limited to anomalous dispersion decreasing fibre and generation of as broad and flat a spectrum as possible [1, 12–14]. Interesting results were obtained in a study of laser pulse compression in normal dispersion increasing fibre [15].

Modern optical fibre drawing technologies allow one to produce essentially arbitrary (e.g., periodic [16]) longitudinal profiles of dispersion parameters. In such fibres, possibilities of supercontinuum generation can be substantially enriched. For example, it is possible to generate polychromatic dispersive radiation in a specially designed fibre with a longitudinal variation in zero dispersion wavelength (ZDW) corresponding to a Raman redshift of a soliton pump pulse [17] or in fibre with an axially oscillating profile that allows a generating soliton pulse to repeatedly approach the ZDW [18]. The conditions thus created lead to the multiplication of resonance generation points throughout the fibre length and are favourable for an essentially complete pulse energy conversion to light with a broad dispersion spectrum.

This paper presents a continuation of our studies concerned with the transformation of the spectrum of an input telecom pulse in fibres with different variations in their longitudinal dispersion profile with the aim of transforming it and bringing it to the preset range of 2–2.5 μm, while maintaining the pulsed character of the radiation.

2. Model

The purpose of this work is to study how a medium-power laser pulse launched into fibre in its anomalous dispersion range propagates further at a fairly arbitrary variation in dispersion along the length of the fibre. First, we restrict our

I.O. Zolotovskii, D.A. Korobko, D.A. Stoliarov Ulyanovsk State University, ul. L. Tolstogo 42, 432017 Ulyanovsk, Russia; e-mail: korobkotam@rambler.ru;
V. Rastogi Indian Institute of Technology Roorkee, Uttarakhand, India
A.A. Sysolyatin A.M. Prokhorov General Physics Institute, Russian Academy of Sciences, ul. Vavilova 38, 119991 Moscow, Russia

Received 7 May 2018; revision received 17 June 2018
Kvantovaya Elektronika **48** (9) 813–817 (2018)
Translated by O.M. Tsarev

consideration to so-called flattened dispersion fibres, whose characteristic feature is that their third-order dispersion (TOD) is small in magnitude and changes sign. Such fibres can be produced by varying their outer diameter [19] using both photonic crystal fibres with a broad transmission spectrum (300–2500 nm, depending on fibre structure) and standard telecom W-profile silica fibre preforms. The latter type was chosen as model fibre. Figure 1 shows dispersion curves of W-profile fibres at several outer cladding diameters. It can be seen that the spectral range of anomalous dispersion in this type of fibre is bounded by two zero dispersion points.

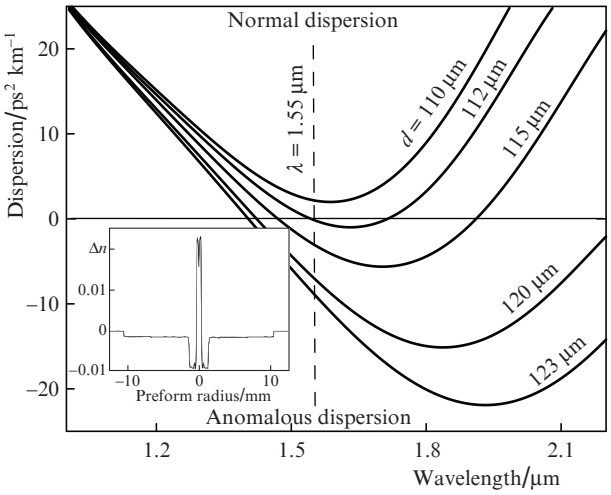

Figure 1. Calculated dispersion curves of flattened dispersion fibres at several outer cladding diameters d. Inset: refractive index profile of the preform used to fabricate the flattened dispersion fibres.

Light propagation through fibre was modelled using the generalised nonlinear Schrödinger equation (NLSE) for the $A(z, t)$ field amplitude, taking into account both higher order dispersion terms (up to the seventh order: $k \leqslant 7$) and higher order nonlinear factors, namely, SRS and nonlinearity dispersion [1]:

$$\frac{\partial A}{\partial z} - \sum_{k\geqslant 2} \frac{\mathrm{i}^{k+1}}{k!}\beta_k(z)\frac{\partial^k A}{\partial t^k} = \mathrm{i}\gamma\left(1 + \mathrm{i}\frac{1}{\omega_0}\frac{\partial}{\partial t}\right)\left[A\int_{-\infty}^{\infty} R(t')\left|A(z,t-t')\right|^2 \mathrm{d}t'\right]. \quad (1)$$

Here ω_0 is the carrier frequency corresponding to the wavelength $\lambda = 1.55$ μm and

$$R(t) = 0.82\delta(t) + 0.18\frac{\tau_1^2 + \tau_2^2}{\tau_1\tau_2^2}\exp\left(-\frac{t}{\tau_2}\right)\sin\left(\frac{t}{\tau_1}\right)\Theta(t)$$

is the Raman response function, where the parameters $\tau_1 = 12.2$ fs and $\tau_2 = 32$ fs correspond to the response of silica fibre; $\Theta(t)$ is the Heaviside function; and $\delta(t)$ is the delta function. The dispersion parameters $\beta_k(z)$ [where β_2 is group velocity dispersion (GVD); β_3 is TOD; etc.; $k \leqslant 7$] are determined by the longitudinal cladding diameter profile, $d(z)$. Their values at the diameters indicated in Fig. 1 were obtained by fitting dispersion curves and taken as references (for example, at $d = 115$ μm we have $\beta_2 = -2.963$ ps^2 km^{-1}, $\beta_3 = 0.04275$ ps^3 km^{-1}, $\beta_4 = 1.882\times10^{-4}$ ps^4 km^{-1}, $\beta_5 = -2.69\times10^{-6}$ ps^5 km^{-1}, $\beta_6 = 1.928\times10^{-8}$ ps^6 km^{-1} and $\beta_7 = -6.287\times10^{-11}$ ps^7 km^{-1}). For the other $d(z)$ values, dispersion parameters can be evaluated using quadratic interpolation. The Kerr nonlinearity coefficient γ is a weak function of outer cladding diameter. In the approximation taken here, it is constant along the length of the fibre ($\gamma = 6$ W km^{-1}).

The key physical effect determining the formation of a supercontinuum in optical fibre is the generation of resonance dispersive radiation. A condition for low-amplitude dispersive wave generation at frequency ω_{DW} is phase matching between the generating soliton and dispersive radiation: $\beta_{\mathrm{s}}(\omega_{\mathrm{DW}}) = \beta_{\mathrm{DW}}(\omega_{\mathrm{DW}})$, where β_{s} and β_{DW} are the soliton and dispersive wave propagation constants. This condition can be represented in the form [13, 17]

$$\sum_{k\geqslant 2}\frac{\beta_k(\omega_0)}{k!}(\omega_{\mathrm{DW}} - \omega_0)^k = \beta_{\mathrm{s}0} + \beta_{\mathrm{s}1}(\omega_{\mathrm{s}})(\omega_{\mathrm{DW}} - \omega_{\mathrm{s}}) + \frac{\gamma P}{2}, \quad (2)$$

where $\beta_{\mathrm{s}1}(\omega_{\mathrm{s}})$ is the inverse group velocity of the soliton at its frequency ω_{s} and P is the soliton pulse peak power. In Fig. 2, the generation condition is illustrated for two cases: (1) $\lambda_{\mathrm{s}} = 1.6$ μm and the soliton is located in a fibre section of diameter $d = 120$ μm; (2) $\lambda_{\mathrm{s}} = 1.75$ μm and $d = 115$ μm. Let a pulse propagate through a fibre with a monotonically decreasing diameter [for simplicity, the peak power P is taken to be 500 W in both cases and the pulse duration is $\tau_{\mathrm{s}} = (|\beta_2|/\gamma P)^{1/2} \approx 100$ fs], undergoing a Raman redshift from an initial carrier wavelength $\lambda = 1.55$ μm. In the former case, there are then conditions for the generation of resonance dispersive radiation with $\lambda_{\mathrm{DW}} \approx 1.2$ μm and a spectral intensity proportional to the intensity in the spectrum of the soliton at this frequency: $\propto \mathrm{sech}^2[\pi(\omega_{\mathrm{s}} - \omega_{\mathrm{DW}})\tau_{\mathrm{s}}]$ [20]. For a transform-limited soliton with $\tau_{\mathrm{s}} = 100$ fs, the intensity of the dispersive radiation generated at 1.2 μm is estimated at about –20 dB of the peak power in the spectrum of the soliton (another intersection, beyond Fig. 2, corresponds to generation of negligible intensity because of the large frequency difference). In the latter case, the generation of two resonance radiation bands, with $\lambda_{\mathrm{DW}} \approx$

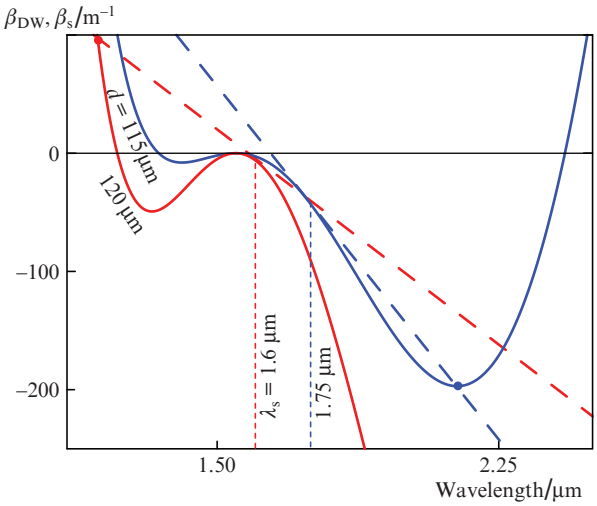

Figure 2. Schematic of dispersive radiation generation by a soliton at two carrier wavelengths λ_{s} in fibre sections differing in diameter. The solid and dashed lines represent the $\beta_{\mathrm{DW}}(\lambda)$ and $\beta_{\mathrm{s}}(\lambda)$ data. The filled circles represent the points where the phase matching condition (2) is fulfilled.

1.1 μm (beyond Fig. 2) and $\lambda_{DW} \approx 2.2$ μm, is also possible, and the intensity of the latter band is considerably higher. As a result, it would be expected that pulse propagation in a fibre of decreasing diameter would be accompanied by the excitation of two resonance radiation bands of variable intensity, connected to the two zero dispersion points: inflection points in the $\beta_{DW}(\lambda)$ curves.

It follows from the above that the problem formulated by us is to examine the transformation of the spectrum of a laser pulse launched into optical fibre and optimise the longitudinal profile $d(z)$ of the fibre so as to ensure sufficient intensity of the transformed spectrum in the desired spectral range.

3. Generation of soliton pulses with a carrier wavelength above 2 μm

The problem formulated above can be concretised as follows: we try to find longitudinal fibre diameter profiles, $d(z)$, that allow soliton pulses forming when an input telecom signal is launched into the fibre to be Raman-shifted to the wavelength range $\lambda > 2$ μm, while minimising the soliton energy loss. An obvious consequence is that the soliton propagation spectrum should have anomalous dispersion. From the well-known relation for the rate of the Raman shift of the soliton frequency [21], $d\Omega/dz \propto \beta_2/\tau_s^4$, the rate of the Raman shift in dispersion varying fibre can easily be estimated. Assuming that soliton parameters vary adiabatically, remaining connected to each other, $|D|/\tau_s = \gamma E/2$ (where E is the soliton energy), we obtain

$$\frac{d\Omega}{dz} \propto \frac{\gamma E}{2}\frac{1}{\tau_s^3} = \frac{\gamma^4 E^4}{16|D(z)|^3}. \quad (3)$$

This relation refers to dispersion D (ps^2 km^{-1}) 'local' in frequency, i.e. it takes into account changes in dispersion due not only to the variation in diameter, $d(z)$, but also to the variation in carrier frequency during pulse propagation through $d(z) = \text{const}$ fibre (Fig. 1).

At first glance, it might be inferred from the relation $d\Omega/dz \propto D^{-3}$ that, to ensure a large Raman shift, it would be sufficient to launch a pulse into a low anomalous dispersion fibre and then find a $d(z)$ profile such that the Raman shift of the soliton would not lead to a rise in dispersion. Thus, one can obtain a flat-dispersion tapered fibre. Consider the following example: A transform-limited Gaussian pulse at a wavelength of 1550 nm of duration $\tau_0 = 0.3$ ps and 250 W peak power is launched into fibre with an initial diameter $d = 115.5$ μm (Fig. 3). The fibre has a constant diameter $d(z) = 115.5$ μm and anomalous dispersion $\beta_2 = -3.7$ ps^2 km^{-1} over its first 20 m. In this section, the input pulse breaks up into a fundamental soliton with the maximum peak power and a Raman redshift and residual radiation near the pump frequency (its peak power is considerably lower, so the Raman shift is negligible). In addition, in this section the soliton shifts to the right and passes through a minimum in the dispersion curve (Fig. 1). Then, the fibre diameter increases so that the dispersion of the fibre at the fundamental soliton frequency ω_s,

$$\beta_2(\omega_0) + \sum_{k>2} \frac{\beta_k(\omega_0)(\omega_s - \omega_0)^{k-2}}{(k-2)!},$$

remains constant. Since this condition is fulfilled in the fibre of increasing diameter, the spectrum of the fundamental soliton evolves at a constant distance from the second, 'red' zero

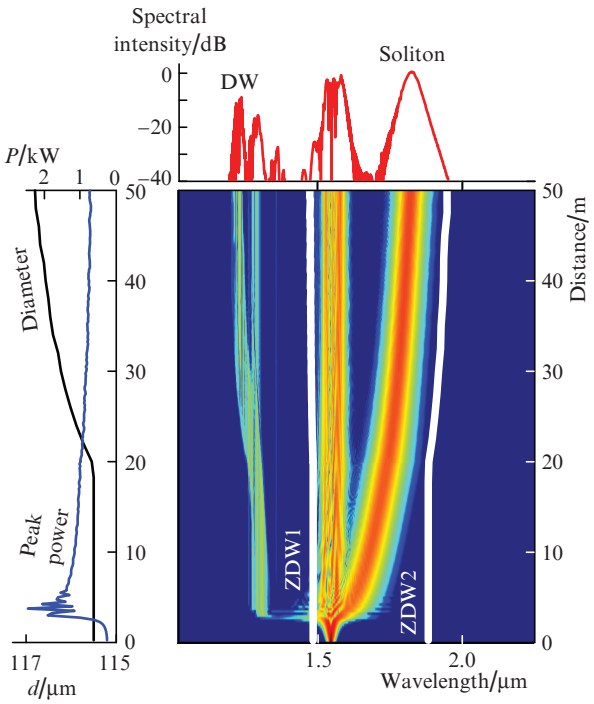

Figure 3. Evolution of the spectrum of an input pulse in a fibre of increasing diameter. Left panel: variations of fibre diameter and peak power along the length of the fibre. Top panel: emission spectrum at the fibre output. DW: spectrum of dispersive radiation; ZDW1 and ZDW2: zero dispersion wavelengths.

dispersion wavelength ZDW2 (Fig. 3). Because the resonance generation point is steadily red-shifted with increasing fibre diameter, the intensity of the soliton spectrum at this point remains insignificant throughout the length of the fibre and there is no appreciable soliton energy conversion to the dispersion spectrum in the longer wavelength normal dispersion region (to the right of ZDW2).

Owing to the constant dispersion at the carrier frequency of the soliton, its spectral width remains unchanged during propagation and its peak power varies insignificantly. However, the small amount of dispersion in the input fibre segment creates good conditions for resonance radiation generation in the shorter wavelength normal dispersion region (to the left of ZDW1). Even in the input fibre segment, with input pulse compression before fundamental soliton formation, we notice dispersive radiation generation, and the high peak power of the compressed pulse leads to considerable energy removal from the input pulse, owing to which the rate of its Raman shift also decreases [see relation (3)]. As a result, at a fibre length of the order of hundreds of metres it is essentially impossible to obtain a pulse with a wavelength above 2 μm by the method in question. The resultant spectrum has the form of a band nonuniform in intensity between 1.3 and 2 μm.

We propose a slightly different configuration for efficient pulse generation at wavelengths above 2 μm. The input fibre segment should have a larger diameter and, accordingly, higher anomalous dispersion. This will make it possible, first, to avoid short-wavelength resonance generation in the initial stage and, second, to produce a higher energy fundamental soliton because the soliton order of the input pulse meets the relation $N \propto |\beta_2|^{-1/2}$ [22], so the higher the initial dispersion, the higher the fraction of the input pulse energy transferred to

the fundamental soliton. In this case, however, after passing the input fibre segment the soliton is located to the left of the minimum in the dispersion curve for a given initial diameter (Fig. 1). After this segment, the fibre diameter should first decrease (to avoid a rise in anomalous dispersion and prevent a reduction in soliton peak power) and then increase, by analogy with the case considered above, in order to maintain roughly constant dispersion at the carrier frequency of the soliton.

Figure 4 presents a model implementation of this configuration. The input pulse is the same as in the above example: transform-limited Gaussian pulse of duration $\tau_0 = 0.3$ ps with a 250 W peak power. In the input fibre segment 11 m in length, with $d = 128.5$ μm ($\beta_2 \approx -17$ ps^2 km^{-1}), a fundamental soliton separates from it. Note that there is no resonance generation in this case. In the next fibre segment, about 100 m in length, the fibre diameter decreases.

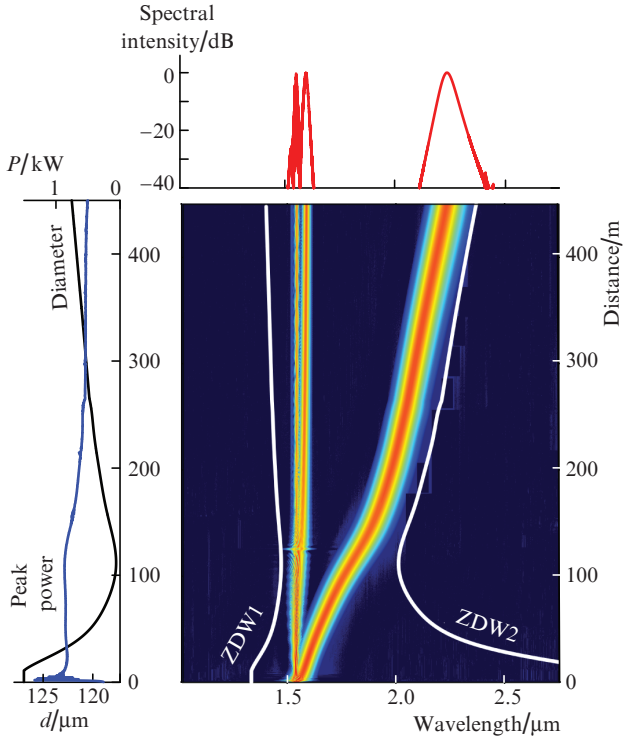

Figure 4. Evolution of the spectrum of an input pulse in a fibre with a special longitudinal profile. Left panel: variations of fibre diameter and peak power along the length of the fibre. Top panel: emission spectrum at the fibre output.

In this case, the fibre diameter profile is such that the soliton peak power remains roughly constant upon a Raman shift. It is important that, in this segment, the soliton surmount the frequency minimum in the dispersion curve while red-shifting. After a short transition zone, the fibre diameter gradually rises in the next segment, ensuring constant dispersion at the carrier wavelength of the soliton. It is worth noting that, as in the above example, the soliton peak power is approximately constant in this segment. As a result, a 450-m-long fibre has a spectrum with more than 60% of its energy lying in the range 2.2–2.3 μm. An important point is that, as distinct from a number of converters [4, 8–10, 23] that transform the spectrum of a pump pulse into a broad supercontinuum in the range 1.6–2.5 μm, which contains, among other things, a broadband dispersive component, in the proposed configuration such energy, concentrated in the desired range, is accounted for by a single subpicosecond pulse (about 120 fs in duration, with a peak power $P = 440$ W), which is potentially attractive for a number of applications.

Note also that, if necessary, the longitudinal profile of fibre can be modified for converting an output soliton pulse to spectrally flat dispersive radiation. To this end, one should merely butt-join an about 10-m length of fibre with a monotonically decreasing diameter to the fibre under consideration. The decrease in diameter should be such that dispersion at the pulse carrier frequency changes sign. Crossing ZDW2 during propagation through such an output fibre segment, a soliton pulse transforms into broadband dispersive radiation [17]. The present modelling results indicate that the resultant subpicosecond pulse converts into spectrally flat radiation in the range 2–2.4 μm.

A drawback to the proposed method is that fibre with a specially calculated longitudinal profile is only suitable for one type of input pulse (in the above example, the fibre profile corresponds to a transform-limited Gaussian pulse of specified power and duration). At the same time, in the case of a configuration comprising one telecom pulse source and fibre with an appropriate longitudinal profile, this drawback should not restrict the application field of this approach to the generation of subpicosecond pulses in the 2 μm range.

4. Conclusions

We have considered the evolution of the spectrum of a medium-power input telecom laser pulse during propagation in a longitudinally inhomogeneous flattened dispersion silica fibre. Using modelling results, we have found an optimal longitudinal fibre diameter profile ensuring transfer of more than 60% of the input pulse energy to a subpicosecond pulse in the range 2.2–2.3 μm. The resultant soliton pulse is spectrally well separated from the other components and can readily be filtered off for direct use in applications or further amplification using holmium or thulium fibre amplifier systems. In the near future, we plan to fabricate several optical fibres with the above configuration and experimentally verify the proposed method.

Acknowledgements. This work was supported by the Russian Science Foundation (Project No. 16-42-02012). D.A. Stoliarov received support from the Russian Foundation for Basic Research (Grant No. 17-302-50024 'mol_nr').

References

1. *Supercontinuum Generation in Optical Fibers*. Ed. by J.M.Dudley, J.R.Taylor (Cambridge: Cambridge University Press, 2010).
2. Dianov E.M., Kryukov P.G. *Quantum Electron.*, **31** (10), 877 (2001) [*Kvantovaya Elektron.*, **31** (10), 877 (2001)].
3. Zheltikov A.M. *Phys. Usp.*, **49** (6), 605 (2006) [*Usp. Fiz. Nauk*, **176** (6), 623 (2006)].
4. Kamynin V.A., Kurkov A.S., Tsvetkov V.B. *Quantum Electron.*, **41** (11), 986 (2011) [*Kvantovaya Elektron.*, **41** (11), 986 (2011)].
5. Buczynski R., Bookey H.T., Pysz D., Stepien R., Kujawa I., McCarthy J.E., Taghizadeh M.R. *Laser Phys. Lett.*, **7** (9), 666 (2010).
6. Chamorovskiy A., Marakulin A.V., Ranta S., Tavast M., Rautiainen J., Leinonen T., Kurkov A.S., Okhotnikov O.G. *Opt. Lett.*, **37**, 1448 (2012).
7. Kivisto S., Hakulinen T., Guina M., Okhotnikov O.G. *IEEE Photonics Technol. Lett.*, **19** (12), 934 (2007).

8. Xia C., Kumar M., Kulkarni O.P., Islam M.N., Terry F.L. Jr., Freeman M.J., Mazé G. *Opt. Lett.*, **31** (17), 2553 (2006).
9. Kurkov A.S., Sholokhov E.M., Sadovnikova Y.E. *Laser Phys. Lett*., **8** (8), 598 (2011).
10. Anashkina E.A., Andrianov A.V., Koptev M.Yu., Mashinsky V.M., Muravyev S.V., Kim A.V. *Opt. Express*, **20**, 27102 (2012).
11. Mori K., Takara H., Kawanishi S., Saruwatari M., Morioka T. *Electron. Lett*., **33**, 1806 (1997).
12. Genty G., Coen S., Dudley J.M. *J. Opt. Soc. Am. B*, **24** (8), 1771 (2007).
13. Korobko D.A., Okhotnikov O.G., Stoliarov D.A., Sysolyatin A.A., Zolotovskii I.O. *J. Opt. Soc. Am. B*, **32** (4), 692 (2015).
14. Zolotovskii I.O., Korobko D.A., Okhotnikov O.G., Stolyarov D.A., Sysolyatin A.A. *Quantum Electron*., **45** (9), 844 (2015) [*Kvantovaya Elektron*., **45** (9), 844 (2015)].
15. Korobko D.A., Okhotnikov O.G., Stoliarov D.A., Sysoliatin A.A., Zolotovskii I.O. *J. Lightwave Technol*., **33** (17), 3643 (2015).
16. Sysoliatin A.A., Dianov E.M., Konyukhov A.I., Melnikov L.A., Stasyuk V.A. *Laser Phys*., **17** (11), 1306 (2007).
17. Milián C., Ferrando A., Skryabin D.V. *J. Opt. Soc. Am. B*, **29**, 589 (2012).
18. Bendahmane A., Braud F., Conforti M., Barviau B., Mussot A., Kudlinski A. *Optica*, **1** (4), 243 (2014).
19. Akhmetshin U.G., Bogatyrev V.A., Senatorov A.K., Sysolyatin A.A., Shalygin M.G. *Quantum Electron*., **33** (3), 265 (2003) [*Kvantovaya Elektron*., **33** (3), 265 (2003)].
20. Skryabin D.V., Luan F., Knight J.C., Russell P.S. *Science*, **301**, 1705 (2003).
21. Gordon J.P. *Opt. Lett*., **11**, 662 (1986).
22. Agrawal G.P. *Nonlinear Fiber Optics* (London: Academic, 1995; Moscow: Mir, 1996).
23. Kamynin V.A., Kurkov A.S., Mashinsky V.M. *Laser Phys. Lett.*, **9** (3), 219 (2012).